

Creep Behavior of ABS Polymer in Temperature–Humidity Conditions

Teagen An, Ramya Selvaraj, Seokmoo Hong, and Naksoo Kim

(Submitted April 14, 2016; in revised form March 30, 2017; published online April 20, 2017)

Acrylonitrile-Butadiene-Styrene (ABS), also known as a thermoplastic polymer, is extensively utilized for manufacturing home appliances products as it possess impressive mechanical properties, such as, resistance and toughness. However, the aforementioned properties are affected by operating temperature and atmosphere humidity due to the viscoelasticity property of an ABS polymer material. Moreover, the prediction of optimum working conditions are the little challenging task as it influences the final properties of product. This present study aims to develop the finite element (FE) models for predicting the creep behavior of an ABS polymeric material. In addition, the material constants, which represent the creep properties of an ABS polymer material, were predicted with the help of an interpolation function. Furthermore, a comparative study has been made with experiment and simulation results to verify the accuracy of developed FE model. The results showed that the predicted value from FE model could agree well with experimental data as well it can replicate the actual creep behavior flawlessly.

Keywords Acrylonitrile-Butadiene-Styrene (ABS), creep behavior, humidity, temperature, viscoelasticity property

1. Introduction

Home appliances, produced utilizing Acrylonitrile-Butadiene-Styrene (ABS) polymers, are exposed to certain temperature and humidity levels based on their operating environments. When exposed to the aforementioned environments for a long time, permanent deformation may occur, leading to inadmissible external appearance or product malfunctions. For this reason, it is necessary to predict the deformation of ABS polymer material under environmental changes and to optimize the product design based on the creep deformation behavior.

In the literature, several researchers have investigated the creep behavior of polymeric material in different ways. Yin et al. (Ref 1) studied the deformation behavior of the alloys of polycarbonate (PC) and acrylonitrile-butadiene-styrene (ABS) at elevated temperatures and high strain rates. Chen et al. (Ref 2) discussed the effect of relative humidity on the uniaxial cyclic softening/hardening and intrinsic heat generation of polyamide-6 polymer. Dreher et al. (Ref 3) examined the creep behavior of polymeric material, such as poly-lactic-lactide (PLLA) and poly-lactic-co-glycolide (PLGA), concluding that the creep strain rate mainly depends on the applied weight. Solasi et al. (Ref 4) inspected creep behaviors of the polymer material commonly used for fuel cell applications by utilizing different operating temperature and humidity levels, stating that

creep deformation of polymer material is insignificant at the lower temperature and humidity levels. Vlahinic et al. (Ref 5) examined the creep rate of viscous materials containing with moisture content, and the results revealed that the creep rate is affected by moisture concentration.

In this paper, finite element (FE) methodology has been utilized for the prediction of the permanent deformation in ABS polymer material and the results have been validated with laboratory experiments. In order to properly describe the behavior of the ABS material, a two-layer viscoelastic-plastic model has been initially used (Ref 6-8) and afterward modified in order to include also the creep effect. As it will be proved in the paper, the new developed model better represents the behavior of the ABS polymer material than those in the literature, since also the strain rate influence is included in the model. Mechanical and the creep properties have been determined by tensile and creep experimental tests, and the results have been used for the description of the material behavior and for the calculation of the material model constants. For the validation of the developed model, a blade-shaped specimen has been used and tested under different temperature and humidity conditions. The results of the test have been compared with those of the developed model, showing how the proposed procedure can accurately predict the creep effect in a short amount of time.

2. Material Model

2.1 Mechanical Property

The deformation of viscoelastic polymeric material cannot be easily expressed using general rigid plastic or elastic-plastic material models. Therefore, a material model that can simultaneously consider viscoelastic and elastic-plastic property of polymeric materials is necessary.

Kusoglu et al. (Ref 9) and Tang et al. (Ref 10) used the von Mises yield criterion with isotropic hardening to represent the mechanical property of a polymeric material and inferred that

Ramya Selvaraj and Naksoo Kim, Department of Mechanical Engineering, Sogang University, Seoul 121-742, Korea; Teagen An, Digital Appliances Business, Samsung Electronics Co., Ltd., 129, Samsung-ro, Yeongtong-gu, Suwon-si, Gyeonggi-do 443-742, Korea; and Seokmoo Hong, Department of Metallic Mold Design Engineering, Konju National University, Gongju, Chungnam-do 31080, Korea. Contact e-mail: nskim@sogang.ac.kr

both mechanical properties and plastic deformation are affected by different temperature and humidity conditions. Tervoort et al. (Ref 11) defined the mechanical property of a polymeric material as a nonlinear viscoelastic behavior and considered yield dependency on strain rate.

The two-layer viscoelastic-plastic model simultaneously considers viscoelastic and elastic-plastic properties of material (Ref 6-8, 12). It consists of a parallel combination of a time-dependent viscoelastic layer and an elastic-plastic time-independent layer, as shown in Fig. 1. Here Fig. 1 expresses the deformation of ABS (Ref 10). Whereas K_p , K_v , H denotes the elastic modulus of the elastic-plastic layer and the viscoelastic layer and the hardness coefficient of the plastic region, respectively. The yield stress defined as σ_y , and A , n are the material constants of the viscous region.

Due to the structure of the considered material model, Fig. 1, the total mechanical strain ϵ_{ij}^M assumes the same value on both layer, Eq 1, where ϵ_{ij}^{EV} is related to the viscoelastic layer regions, whereas ϵ_{ij}^{EP} to the elastic-plastic layer.

$$\epsilon_{ij}^M = \epsilon_{ij}^{EV} = \epsilon_{ij}^{EP} \quad (\text{Eq 1})$$

The strain of the elastic-plastic layer can be expressed as the sum of the linear elastic strains of spring elements, $(\epsilon_{ij}^{EP})_{el}$, and the plastic strain, $(\epsilon_{ij}^{EP})_{pl}$, as shown in Eq 2. The strain of the elastic region in Eq 2 is expressed as shown in Eq 3.a in accordance to the isotropic Hooke's law, and the equivalent plastic strain from the strain increment, $d(\epsilon_{ij}^{EP})_{pl}$, of the plastic region is expressed as shown in Eq 3.b.

$$\epsilon_{ij}^{EP} = (\epsilon_{ij}^{EP})_{el} + (\epsilon_{ij}^{EP})_{pl} \quad (\text{Eq 2})$$

$$(\epsilon_{ij}^{EP})_{el} = \frac{1+\nu}{K_p} \sigma_{ij}^{EP} - \frac{\nu}{K_p} \delta_{ij} \sigma_{kk}^{EP} \quad (\text{Eq 3.a})$$

$$(\epsilon_{ij}^{EP})_{pl} = \int \sqrt{\frac{2}{3}} d(\epsilon_{ij}^{EP})_{pl} d(\epsilon_{ij}^{EP})_{pl} \quad (\text{Eq 3.b})$$

The total strain in the viscoelastic layer is the sum of elastic strain, $(\epsilon_{ij}^{EV})_{el}$, and the viscous strain, $(\epsilon_{ij}^{EV})_{vi}$, in Eq 4. Similarly in the elastic-plastic layer, elastic strain in the viscoelastic layer is defined as Eq 5.a by isotropic Hooke's law. The rate of viscous strain is defined as Eq 5.b by utilizing the Norton-Hoff stress-strain rate law, as proposed in Ref 13. The constants, A and n , represent material parameters in viscous region, as introduced in Fig. 1.

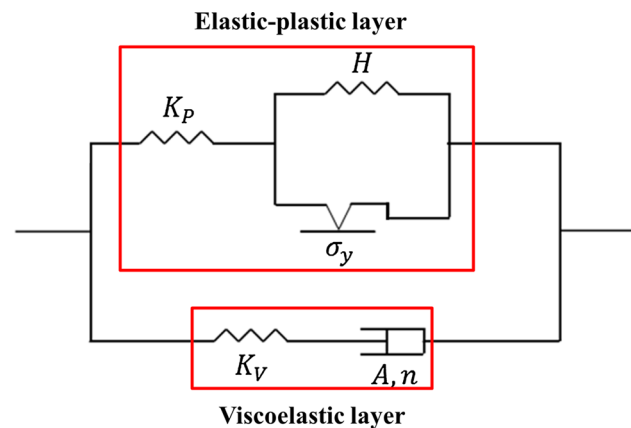


Fig. 1 Idealized one-dimensional representation of the two-layer viscoelastic-plastic model

$$\epsilon_{ij}^{EV} = (\epsilon_{ij}^{EV})_{el} + (\epsilon_{ij}^{EV})_{vi} \quad (\text{Eq 4})$$

$$(\epsilon_{ij}^{EV})_{el} = \frac{1+\nu}{K_v} \sigma_{ij}^{EV} - \frac{\nu}{K_v} \delta_{ij} \sigma_{kk}^{EV} \quad (\text{Eq 5.a})$$

$$(\dot{\epsilon}_{ij}^{EV})_{vi} = A (\sigma_{ij}^{EV})^n \quad (\text{Eq 5.b})$$

The total stress, σ is the sum of the stress of viscoelastic layer; σ^{EV} and the stress of elastic-plastic layer; σ^{EP} as shown in Eq 6. The stress of viscoelastic layer is defined as Eq 7.a, the stress of elastic-plastic layer is defined as Eq 7.b. Consequently, the total stress is defined as Eq 8.

$$\sigma = \sigma^{EV} + \sigma^{EP} \quad (\text{Eq 6})$$

$$\sigma^{EV} = \left(\frac{\dot{\epsilon}_o}{A} \right)^{1/n} \quad (\text{Eq 7.a})$$

$$\sigma^{EP} = \sigma_y + H \epsilon^{pl} \quad (\text{Eq 7.b})$$

$$\sigma = \left(\frac{\dot{\epsilon}_o}{A} \right)^{1/n} + \sigma_y + H \epsilon^{pl} \quad (\text{Eq 8})$$

This model is generally used for metal materials in the high-temperature state. The behavior of polymeric material is more sensitive to temperature and strain rate than that of the metallic material. Therefore, the two-layer viscoelastic-plastic model cannot precisely express the behavior of ABS as the strain rate changes, because the behavior is expressed only by the sum of stress components. Since the hardening model for plasticity shown in Eq 8 is too simple to properly describe ABS material behavior, in this study, a modified model for the plastic region is proposed and shown in Eq 9. In the proposed model, H , ϵ_o and n_2 are strain coefficient, whereas A and n_1 are the strain rate coefficients. The validation of the proposed model is shown in following section 3.1.1.

$$\sigma^{EP} = \left(1 + \left(\frac{\dot{\epsilon}}{A} \right)^{\frac{1}{n_1}} \right) \cdot (H \cdot (\epsilon_o + \bar{\epsilon}^{pl})^{n_2}) \quad (\text{Eq 9})$$

2.2 Creep Property

In general, the creep is the tendency of a solid material to deform permanently under the influence of mechanical stresses. Briody et al. (Ref 14) introduced the creep model for polymeric material considering the temperature and time and compared it with the experimental result. Lim et al. (Ref 15) and Kim et al. (Ref 16) attempted to predict the creep behavior of polymeric material by using the FE model with power law creep model. However, they did not consider the effect of humidity on the creep. Bledzki et al. (Ref 17) and Habeger et al. (Ref 18) studied the effect of humidity for the creep of the polymeric material.

In this paper, the power law creep model with time hardening is used as a creep model to express the creep properties of ABS polymer. Such model expresses creep strain rates, $\dot{\bar{\epsilon}}^{cr}$, as shown in Eq 10.a considering time, stress and temperature (Ref 12, 19, 20).

$$\dot{\bar{\epsilon}}^{cr} = C \cdot \bar{\gamma}^{n_c} \cdot t^m \quad (\text{Eq 10.a})$$

$$\bar{\epsilon} = \bar{\epsilon}^{el} + (1-f)\bar{\epsilon}^{pl} + f\bar{\epsilon}^{cr} \quad (\text{Eq 10.b})$$

In Eq 10.a, \bar{q} is the equivalent deviatoric stress, t is the total time, whereas C , m and n_c are creep constants, which can be expressed as the functions of temperature. However, as previously stated, the target of the present research work is to include not only the temperature effect but also the humidity then the constants of the power law creep model must be expressed as function of temperature and humidity.

In Eq 10.b, the total strain $\bar{\epsilon}$ is defined as the summation of the elastic strain $\bar{\epsilon}^{el}$, plastic strain $\bar{\epsilon}^{pl}$ and the creep strain $\bar{\epsilon}^{cr}$. In addition, f is defined as the ratio between K_V to the sum of K_P and K_V . The creep behavior of the ABS polymer may vary depending on the ratio of elastic modulus, K_P and K_V , of the viscoelastic and elastic-plastic layers, respectively, introduced in section 2.1. K_P can be derived through tensile test conducted with strain rates close to 0, whereas K_V can be determined by creep test, where temperature and humidity are considered as variables. The factor f , Eq 11, which represents the ratio between elastic modulus, is calculated based on the results of creep tests (Ref 12).

$$f = \frac{K_V}{K_P + K_V} \quad (\text{Eq 11})$$

3. Experiment and Result

3.1 Determine the Material Properties by Experiments

In this section, in order to determine the material constants of models that can express the behavior of the ABS polymer considering the mechanical and creep properties introduced earlier, a process to minimize difference between test results and simulation results is introduced.

In the case of the two-layer viscoelastic-plastic model, the tensile test was conducted under various temperatures and strain rates. In the case of the power law creep model, the creep test was conducted considering different temperatures, humidity values and loads. The response of displacement load was measured in the tensile test, and the response of time displacement was measured in the creep test. Second-order polynomial objective function was derived based on the response surface method, and the values of the material constants, which minimize the objective functions, were determined as optimum values. Numerical implementations were conducted again to verify the selected optimum values. When the difference between two following iterations is below 1% the optimization is considered to be completed.

The objective functions forms for the tensile tests and the creep tests are defined as shown in Eq 12.a and 12.b, respectively. In these equations, N represents a sampling point, the superscript c represents FE analysis values, the superscript m represents test values, F represents loads, and D represents deflection.

$$\text{Mechanical property: } \phi_o(A, n_1, H, \epsilon, n_2) = \sum_{i=1}^N \left(\frac{F_i^c - F_i^m}{F_i^m} \right)^2 \quad (\text{Eq 12.a})$$

$$\text{Creep property: } \phi_o(C, m, n_c, f) = \sum_{i=1}^N \left(\frac{D_i^c - D_i^m}{D_i^m} \right)^2 \quad (\text{Eq 12.b})$$

3.1.1 Mechanical Property. To determine the material constants of the two-layer viscoelastic-plastic model, the tensile test was conducted by changing temperature and strain rate. The thickness of specimen was 3 mm. The gauge length of specimen for tensile test was 40 mm, and the width was 7 mm as shown in Fig. 2 (Ref 21). Experimental conditions were as follows: temperature (20, 30, 60, 90 °C), tensile speed [10 mm/min (0.004167 s⁻¹), 300 mm/min (0.125 s⁻¹)]. Load-stroke responses were measured in each condition (eight cases).

Those material constants were determined by minimizing the differences between load-displacement responses of the test and those of the simulations. The FE model was implemented in ABAQUS/Implicit, and the element used was C3D20RT (A 20-node thermally coupled brick, tri-quadratic displacement, trilinear temperature, reduced integration).

The simulation results of the conventional model and the simulation results of the modified model were compared with each other to confirm the validity of the proposed material model, as shown in Fig. 3. The material constants derived from the original and modified model are shown in Table 1. In addition, the Poisson ratio of ABS polymer is assumed to be 0.35. According to the comparison of the results in Fig. 3, the reaction force resulting from displacement is more accurately expressed by author's model than the conventional one (Ref 12) in nonlinear regions. In the case of process condition of 90° and 300 mm/min, in the nonlinear region, the difference between test and simulation results, based on the literature model, exceeds 8%. On the other hand, if author's model is utilized, the difference is less than 1% in all cases. Therefore, in this study, the proposed two-layer viscoelastic-plastic model has been chosen to describe the mechanical property of the ABS polymer, considering the effect of temperature.

In addition, the elastic modulus of the elastic-plastic layer, K_B , as previously presented in section 2.2, was derived from the results of the test conducted at a tension speed of 10 mm/min (strain rate 0.004167 s⁻¹). Based on the results of other strain rate 0.125 s⁻¹ and Eq 11, the K_V which is the elastic modulus of the viscoelastic layer was defined (Table 1). The reason is when the strain rate is low in the viscoelastic model, the influence of K_V is hardly considered and the influence of K_P is large.

3.1.2 Creep Property. To define the creep behavior of the ABS polymer, the creep test was conducted in a chamber where temperature and humidity could be controlled to be maintained or changed over time, as shown in Fig. 4(a). The creep tests were conducted by placing a weight on the center of test specimen to induce the creep, as shown in Fig. 4(b). The test specimens shape was made with the following dimensions: 350 mm long, 100 mm wide and 3 mm thick plates. The test time was 100 h, and the vertical displacement (deflection) of

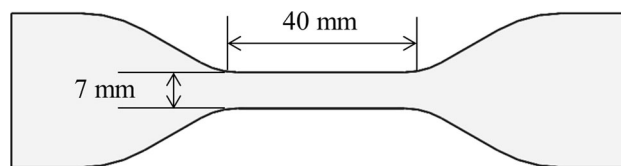


Fig. 2 Shape of ABS specimen used in the tensile test

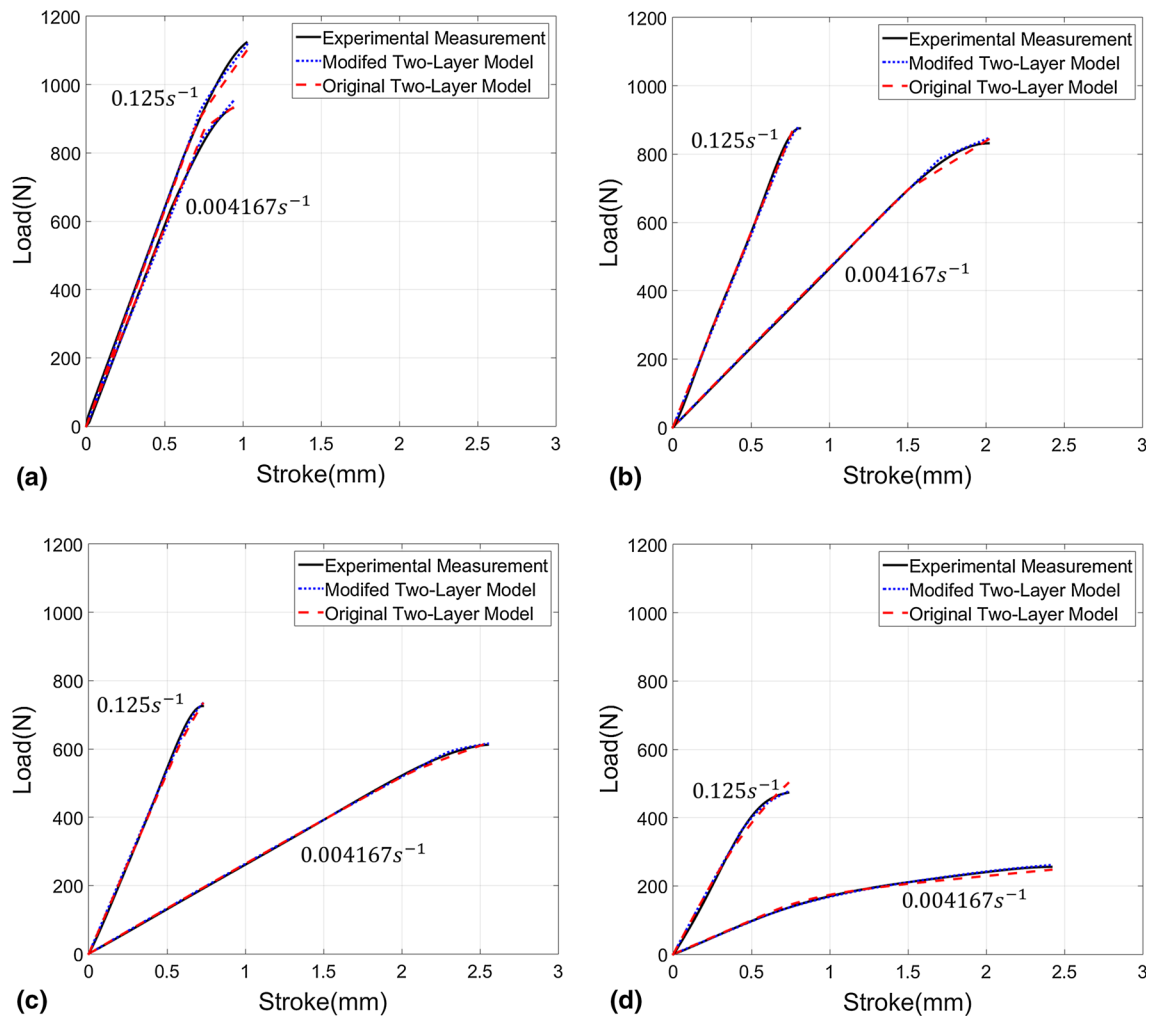


Fig. 3 Comparison between test results and the simulation results obtained through the original model/those obtained through the modified model: (a) 20 °C; (b) 30 °C; (c) 60 °C; (d) 90 °C

Table 1 Constants of original and modified two-layer viscoelastic-plastic model for ABS material

Temperature, °C	σ_Y	A	n	H	Young's modulus, MPa	
					10 mm/min (K_p)	300 mm/min
20	42.02	2.49e-6	3.242	95.323	2280	2480
30	35.09	8.48e-8	4.11	118.48	1382	2195
60	28.2	2.91e-7	2.65	152.1	780	2055
90	6	3.1e-4	1.701	210.2	621	1558

Temperature, °C	A	n_1	H	ϵ_0	n_2	Young's modulus, MPa	
						10 mm/min (K_p)	300 mm/min
20	0.75	0.80	84.978	0.000027	0.071	2280	2480
30	0.65	0.965	74.602	0.00012	0.102	1382	2195
60	0.31	1.212	52.976	0.0021	0.11	780	2055
90	0.01	2.224	10.345	0.0013	0.132	621	1558

the weight was measured as time goes on. The displacement of the weight was measured once every five minutes by using a Pontos 3D (real-time deflection meter) so that nonlinear

displacement could be also smoothly measured. Eighteen different temperature and humidity conditions were tested, as summarized in Table 2.

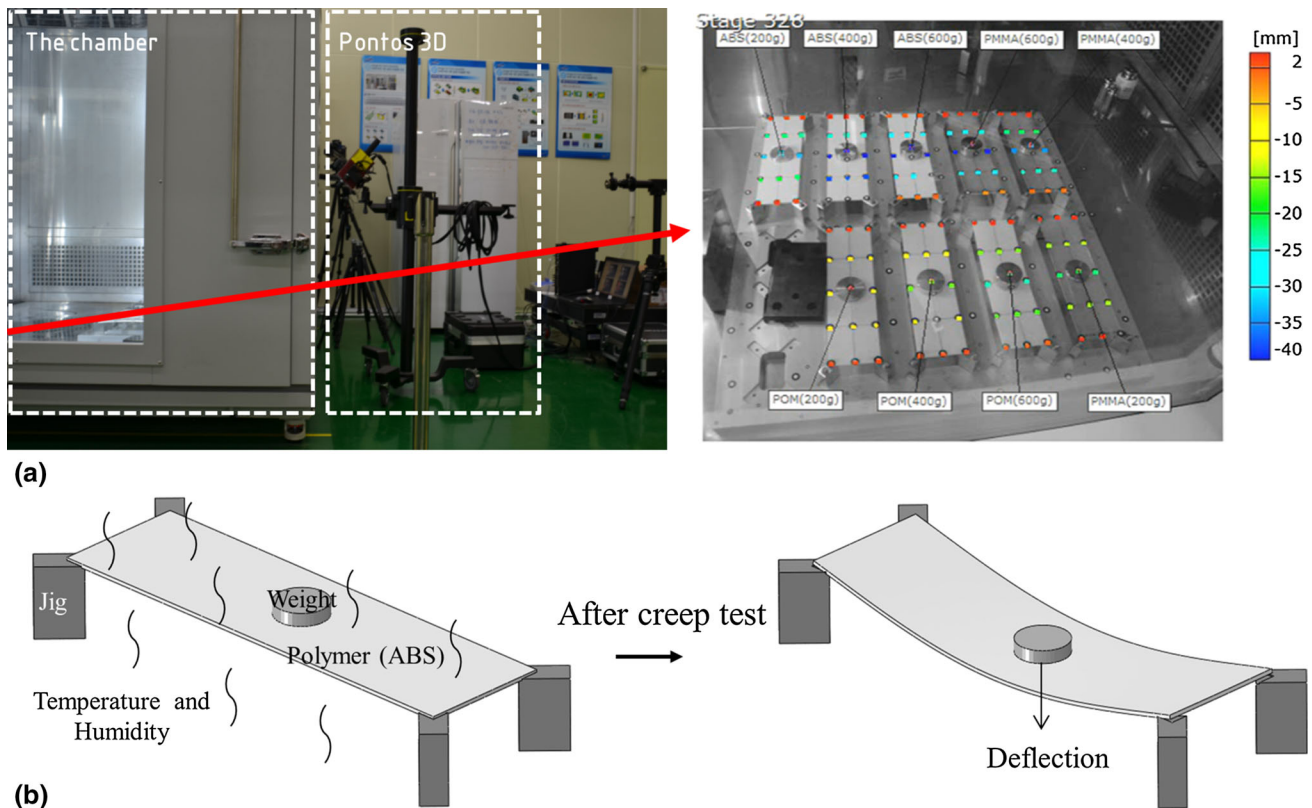


Fig. 4 Test conditions and schematic diagram of creep test: (a) the chamber for creep test and displacement meter; (b) schematic diagram of creep tests of ABS polymer

Table 2 Creep experiment condition about temperature (°C), relative humidity (%) and weight (g)

Temperature, °C	Relative humidity, %	Weight, g
30	0	200
60	45	400
	90	600

Table 3 Thermophysical properties of ABS

Density, kg/mm ³	Specific heat, J/kg·K	Conductivity, W/m·K	Thermal expansion
1.18×10^{-3}	0.177	2050	9.4×10^{-5}

As introduced earlier in section 2.2, the power law creep model with time was used to describe the creep property of the ABS polymer. Four material constants (C , m , n_c and f) were defined by the tests on changing temperature and humidity. A set of temperature and humidity condition was regarded as one case, and material constants (C , m , n_c and f) that minimize the differences between test and simulation results, for different loads, were accordingly derived for the six considered cases (temperature: 30, 60 °C, relative humidity: 0, 45, 90%).

Because of the symmetry of the test specimens and test equipment as shown in Fig. 4, the model was designed as a 1/4 model to secure the efficiency of calculations. The type of element was C3D20RT. In order to accurately simulate the bending displacement along thickness direction, thickness was divided into two layers. The material constants determined

earlier in section 3.1.1 were applied as well as the thermophysical properties, shown in Table 3, were also applied.

The resultant material constants derived by minimizing the value of the objective function are shown in Table 4, and the results of comparison between test and simulation results are shown in Fig. 5. According to the test results on creep, the amount of deflection of the specimens increased as temperature, relative humidity and the load of the weight increased. The error range is defined as 1.89% (for Case 3) and 8.42% (for Case 4), with an average error of 5.3%.

For the Case 4 and Case 5 in Fig. 5, simulation results and experimental results do not match well at the beginning for two reasons: the first reason for this discrepancy is that the convection coefficient was not accurately setup in the simulation, whereas the second one is related to the diffusion coefficient of moisture.

Table 4 Parameters of creep property about temperature and relative humidity

Case	Temperature, °C	Relative humidity, %	<i>C</i>	<i>m</i>	<i>n_c</i>	<i>f</i>
1	30	0	1.03×10^{-7}	-0.461	0.891	0.714
2		45	2.07×10^{-7}	-0.464	0.843	0.727
3		90	4.71×10^{-7}	-0.465	0.843	0.728
4	60	0	1.52×10^{-6}	-0.105	2.713	0.716
5		45	3.2×10^{-6}	-0.15	1.95	0.795
6		90	6.11×10^{-6}	-0.299	1.686	0.904

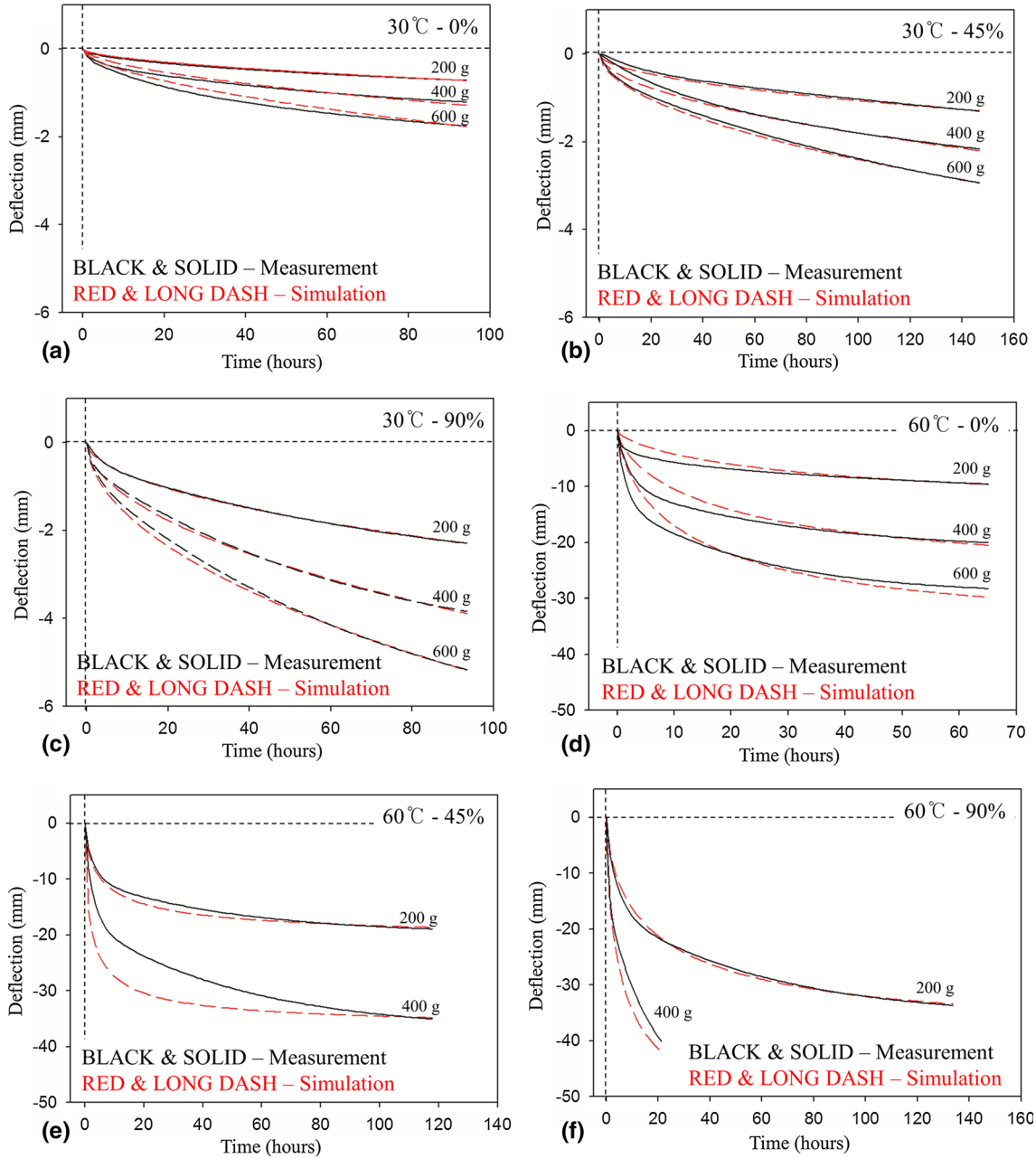


Fig. 5 Comparison of the results of creep tests of the ABS polymer and FE analysis results: (a) Case 1 (30 °C, 0%); (b) Case 2 (30 °C, 45%); (c) Case 3 (30 °C, 90%); (d) Case 4 (60 °C, 0%); (e) Case 5 (60 °C, 45%); (f) Case 6 (60 °C, 90%)

Concerning the diffusion coefficient of moisture, since polymer is a macromolecule and water can enter between molecules, this parameter expresses the rate at which moisture in the atmosphere spreads inside the polymer. Although, in this

paper, the diffusion coefficient of moisture is not taken into account and errors can be seen in the initial part of the curves shown in Fig. 5, at the end of the experiment/simulation time, since the two results converge, it can be inferred that the

influence of the diffusion coefficient of moisture can be neglected without committing a huge error.

Using the creep constants determined from the six combinations of temperature and humidity levels, interpolation function that can predict creep constants for certain temperature and humidity was derived. The interpolation function has to express both nonlinear and linear shape, because C increases as almost linear function of humidity, while other constants increase as its nonlinear function. In addition to that m , n_c and f seems to reach an asymptotic value as humidity increases.

Therefore, the interpolation function which consists of the combination of linear function and exponential function is suggested as Eq 13, whereas the model constants are shown in Table 5.

Based on specific temperature and humidity conditions, the creep constants C , m , n , f can be determined utilizing Eq 13 and the relevant model constants reported in Table 5. In the following section, the proposed function is verified through its application in a FE model of a simple shaped part.

$$C, m, n, f = (a \cdot \text{Humidity}(\%) + b) \cdot e^{(c \cdot \text{Humidity}(\%) + d) \cdot \text{Temperature}(^{\circ}\text{C})} \quad (\text{Eq 13})$$

4. Verification

4.1 Creep Test for Verification of Simple Shape Part

For the model validation, a creep test was conducted on an air conditioner blade and the experiment results were compared to those of ABAQUS/coupled temp-displacement FEM simulations. The blade specimen has been designed with the following dimensions: 800 mm length, 90 mm width, as shown in Fig. 6. In the experiment, as previously explained in section 3.1.2., jigs were placed at both ends of the blade as well as a 200 g weight was placed in the center of the specimen to measure the vertical displacement over time.

The jigs are considered as non-deformable body and defined with discrete rigid elements and fixed at the both ends. The blade is considered as a deformable body and defined with

C3D4T, a linear 4-node fully coupled temperature-displacement element. The blade geometry is discretized into approximately 20,000 elements. Surface film condition interaction, a type of interaction, is created to define the heat transfer from the surface due to convection.

To check the reliability of both FE model and interpolation function, temperature and the humidity conditions, of the experimental environment where the blade was placed, have been randomly varied over time, as illustrated in Fig. 7(a).

For each different test condition, as shown in Fig. 7(a) and summarized in Table 6, the relevant creep constants were calculated by utilizing Eq 13 and inputted in the FE simulation. In the transition zone between one process condition and the following one, the average values to be used for the calculation have been derived and are shown in Fig. 7(b).

For all the FE simulation, apart from the creep model constants, all the remaining material properties have been considered as constant. Moreover, in the FE model, not only the creep deformation is considered but also thermal expansion and plastic deformation due to the applied weight are taken in to account. The comparison between test and FE simulation result is shown in Fig. 8, where the maximum deviation between these two results is calculated in approximately 9% and the trend of the simulated result shows to well follow that of the experiment. In addition, in order to separately evaluate the contribution of humidity and temperature on the blade deflection, constant temperature ranges and three different humidities have been also tested. The results are shown in Fig. 9 where, for each constant temperature interval, 0, 45 and 90% humidity curves are reported, allowing to see the influence of the sole humidity on the blade deflection. On the other hand, following one of the three curves, it is possible to account for the influence of the temperature on the deflection, in case of constant humidity.

The curves are derived by utilizing the proposed numerical model where, for each interval, temperature and humidity have been set to a constant value. The result of each simulation has been inputted in the following one where only the temperature has been varied, whereas the humidity has been kept as constant. By following this procedure, the three different curves for the three different humidity percentages have been derived,

Table 5 Coefficients of creep parameters

Parameter	a	b	c	d
C	4.0×10^{-10}	2.0×10^{-9}	-6.0×10^{-5}	0.0923
m	0.0377	-3.7384	0.0007	-0.0703
n_c	0.0016	0.2786	-0.0002	0.0383
f	-0.0013	0.7076	8.0×10^{-5}	0.0003

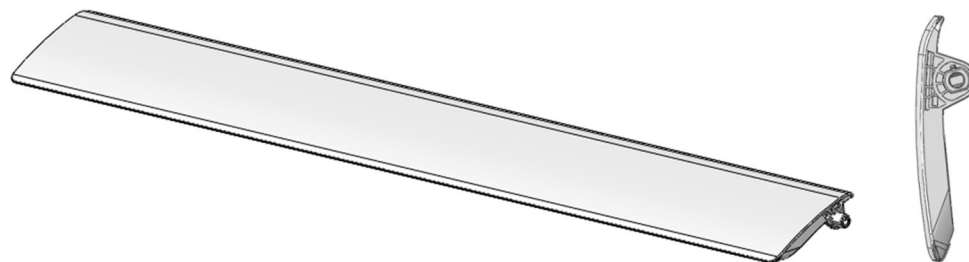


Fig. 6 Blade specimen used to verify the FE model

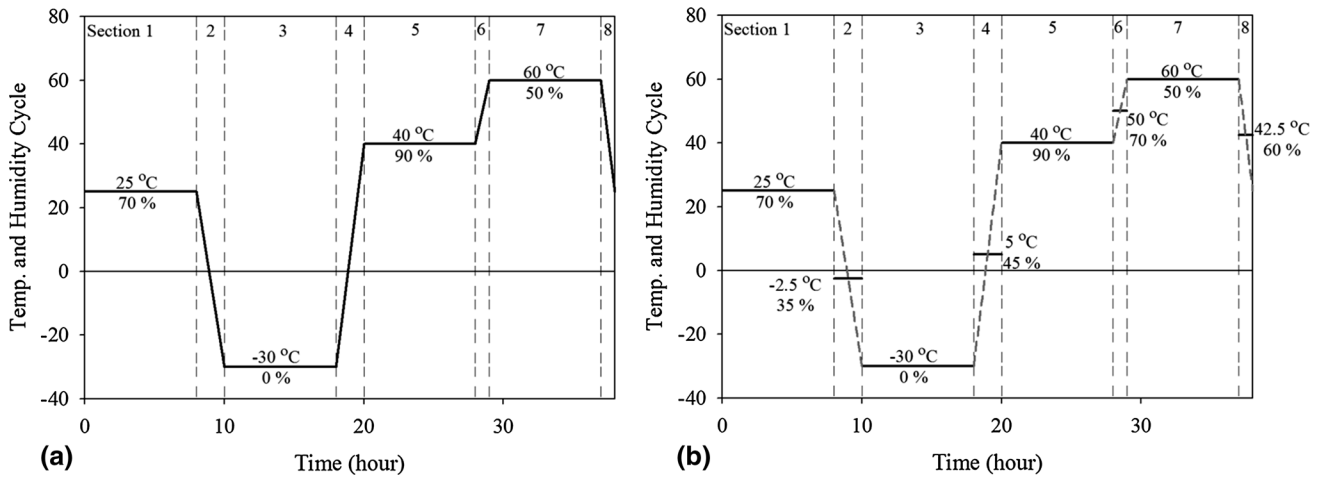


Fig. 7 Temperature and humidity cycle over time used to verify the FE model: (a) temperature and humidity cycle in experiments; (b) temperature and humidity cycle in FE model

Table 6 Temperature and relative humidity in calculation

Section	Time, h	Temperature, °C		Relative humidity, %	
		Experiments	FE model	Experiments	FE model
1	0-8	25	25	70	70
2	8-10	25 to -30	-2.5	70-0	35
3	10-18	-30	-30	0	0
4	18-20	-30 to 40	5	0-90	45
5	20-28	40	40	90	90
6	28-29	40 to 60	50	90-50	70
7	29-37	60	60	50	50
8	37-38	60 to 25	42.5	50-70	60

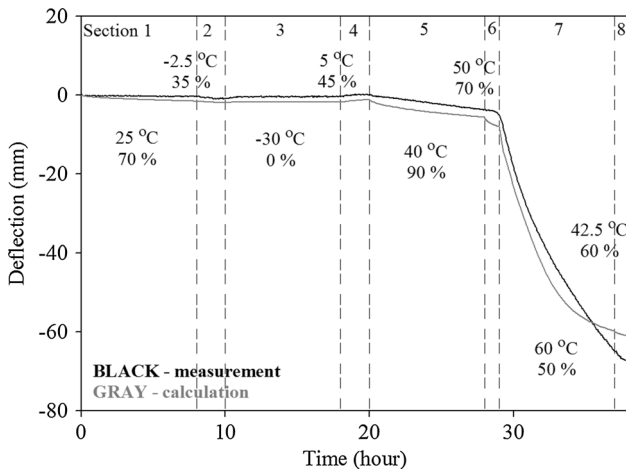


Fig. 8 Comparison of the results of the creep test applied with the temperature and humidity cycle

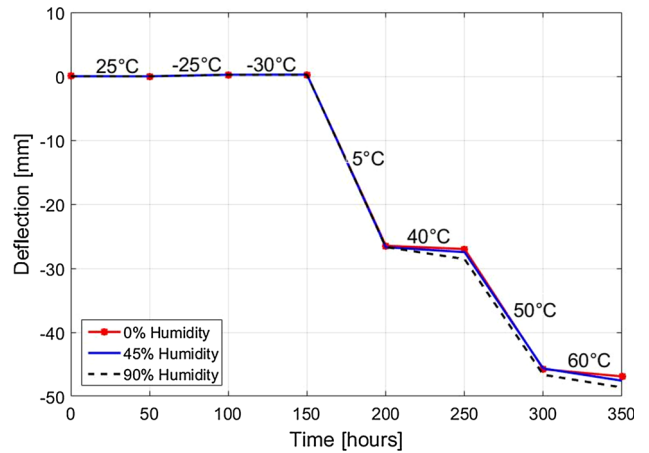


Fig. 9 Constant humidity curves for different constant temperature intervals

allowing to separate the contribution of these two variables on the deflection of the blade.

As shown in Fig. 9, the deflection of the blade is almost negligible in the interval between 25 and -30 °C, but it abruptly decreases when the temperature changes to 5°C, regardless of the humidity percentage. Starting from the

following interval, from 200 h and 40 °C, the influence of the humidity seems to be more significant, with a decreasing deflection as the humidity percentage increases. This behavior is also highlighted in the following two temperature intervals, relevant for 50 and 60 °C.

In conclusion, it can be stated that the humidity plays an important role for relatively high temperatures and times, whereas it is almost negligible for temperatures close to the room temperature or below zero and for relatively short times.

5. Conclusions

Based on the results, it has been proved that the developed model, implemented in the FE simulation, can accurately describe creep behavior of the ABS polymer components those undergo permanent deformation due to the effect of temperature and humidity. A modified two-layer viscoelastic-plastic model was proposed and validated in this paper, and the advantages of its utilization for the description of the viscoelastic behavior of ABS polymer, in comparison with the previous literature model, have been shown. Based on a certain combination of temperature and humidity, the four parameters for the creep model can be calculated and utilized for the estimation of the deflection of the component. The proposed approach has been applied to a simple shape component under different process conditions, showing an error limited to 9% in the estimation of the deflection. In conclusion, based on the results shown in the paper, it can be stated that the developed model can be used to express, with reasonable accuracy, the creep behavior of ABS polymer material under various temperature and humidity conditions.

As concerns future works, based on Zhao et al. (Ref 22) research work, where the stimulus-responsive shape recovery for temperature and humidity after drying has been studied, also the recovery and permanent deformation, after drying, shall be considered.

Acknowledgment

This work was supported by the National Research Foundation of Korea (NRF) grant funded by the Korean Government (NRF-2010-0023152) and Sogang University (Grant no. 201210031)

References

1. Z.N. Yin and T.J. Wang, Deformation of PC/ABS Alloys at Elevated Temperatures and High Strain Rates, *Mater. Sci. Eng. A*, 2008, **29494**, p 304–313
2. K. Chen, G. Kang, F. Lu, J. Chen, and H. Jiang, Effect of Relative Humidity on Uniaxial Cyclic Softening/Hardening and Intrinsic Heat Generation of Polyimide-6 Polymer, *Polym. Test.*, 2016, **56**, p 19–28
3. M.L. Dreher, S. Nagaraja, H. Bui, and D. Hong, Characterization of Load Dependent Creep Behavior in Medically Relevant Absorbable Polymers, *J. Mech. Behav. Biomed. Mater.*, 2014, **29**, p 470–479
4. R. Solasi, X. Huang, and K. Reifsnider, Creep and Stress-Rupture of Nafion® Membranes Under Controlled Environment, *Mech. Mater.*, 2010, **42**, p 678–685
5. I. Vlahinic, J.J. Thomas, H.M. Jennings, and J.E. Andrade, Transient Creep Effects and the Lubricating Power of Water in Materials Ranging from Paper to Concrete and Kevlar, *J. Mech. Phys. Solids*, 2012, **60**, p 1350–1362
6. N.S. Khattri, A.M. Karlsson, M.H. Santare, P. Walsh, and F.C. Busby, Effect of Time-Dependent Material Properties on the Mechanical Behavior of PFSA Membranes Subjected to Humidity Cycling, *J. Power Sources*, 2012, **214**, p 365–376
7. J. Kichenin, K. Van Dang, and K. Boytard, Finite-Element Simulation of a New Two-Dissipative Mechanisms Model for Bulk Medium-Density Polyethylene, *J. Mater. Sci.*, 1996, **31**, p 1653–1661
8. R. Solasi, Y. Zou, X. Huang, and K. Reifsnider, A Time and Hydration Dependent Viscoplastic Model for Polyelectrolyte Membranes in Fuel Cells, *Mech. Time-Depend. Mater.*, 2008, **12**, p 15–30
9. A. Kusoglu, A.M. Karlsson, M.H. Santare, S. Cleghorn, and W.B. Johnson, Mechanical Response of Fuel Cell Membranes Subjected to a Hygro-Thermal Cycle, *J. Power Sources*, 2006, **161**, p 987–996
10. Y. Tang, A.M. Karlsson, M.H. Santare, M. Gilbert, S. Cleghorn, and W.B. Johnson, An Experimental Investigation of Humidity and Temperature Effects on the Mechanical Properties of Perfluorosulfonic acid Membrane, *Mater. Sci. Eng. A*, 2006, **425**, p 297–304
11. T.A. Tervoort, E.T.J. Klompen, and L.E. Govaert, A Multi-mode Approach to Finite, Three-Dimensional, Nonlinear Viscoelastic Behavior of Polymer Glasses, *J. Rheol.*, 1996, **40**, p 779–797
12. ABAQUS, 'ABAQUS Documentation,' Dassault Systèmes, Providence, RI, 2008
13. F.H. Norton, *The Creep of Steel at High Temperatures*, 1st ed., McGraw-Hill Book Company, New York, 1929, p 67–70
14. C. Briody, B. Duignan, S. Jerrams, and S. Ronan, Prediction of Compressive Creep Behaviour in Flexible Polyurethane Foam Over Long Time Scales and at Elevated Temperatures, *Polym. Test.*, 2012, **31**, p 1019–1025
15. S.D. Lim, J.M. Rhee, C. Nah, S.H. Lee, and M.Y. Lyu, Predicting the Long-Term Creep Behavior of Plastics Using the Short-Term Creep Test, *Int. Polym. Process.*, 2004, **19**, p 313–319
16. S.W. Kim, J. Park, E.S. Lee, A Study on Predicting the Long-Term Creep Behavior of Plastics Using the Short-Term Creep Test, 2007, <http://www.simulia.com/forms/world/pdf2007/Kim.pdf>. Accessed 29 January 2015
17. A.K. Bledzki and O. Faruk, Creep and Impact Properties of Wood Fibre–Polypropylene Composites: Influence of Temperature and Moisture Content, *Compos. Sci. Technol.*, 2004, **64**, p 693–700
18. C.C. Habeger, D.W. Coffin, and B. Hojjatie, Influence of Humidity Cycling Parameters on the Moisture-Accelerated Creep of Polymeric Fibers, *J. Polym. Sci. Part B Polym. Phys.*, 2001, **39**, p 2048–2062
19. C.T. Kuo, M.C. Yip, and K.N. Chiang, Time and Temperature-Dependent Mechanical Behavior of Underfill Materials in Electronic Packaging Application, *Microelectron. Reliab.*, 2004, **44**, p 627–638
20. S. Mukherjee and V. Kumar, Numerical Analysis of Time-Dependent Inelastic Deformation in Metallic Media Using the Boundary-Integral Equation Method, *J. Appl. Mech.*, 1978, **45**, p 785–790
21. ASTM D638-14, *Standard Test Method for Tensile Properties of Plastics*, ASTM International, West Conshohocken, PA, 2014
22. Y. Zhao, C. ChunWang, W. MinHuang, and H. Purnawali, Buckling of Poly (methyl methacrylate) in Stimulus-Responsive Shape Recovery, *Appl. Phys. Lett.*, 2011, **99**, p 131911